Journal of Neuroscience Methods 328 (2019) 108446

Contents lists available at ScienceDirect

Journal of Neuroscience Methods

journal homepage: www.elsevier.com/locate/jneumeth

The Quasi-uniform assumption for Spinal Cord Stimulation translational research

Niranjan Khadka[a,*], Dennis Q. Truong[a], Preston Williams[c], John H. Martin[b,c], Marom Bikson[a,*]

[a] Department of Biomedical Engineering, The City College of New York, New York, NY, USA
[b] CUNY Graduate Center, New York, NY, 10031, USA
[c] Department of Molecular, Cellular, and Biomedical Sciences, City University of NY School of Medicine, New York, NY, 10031, USA

GRAPHICAL ABSTRACT

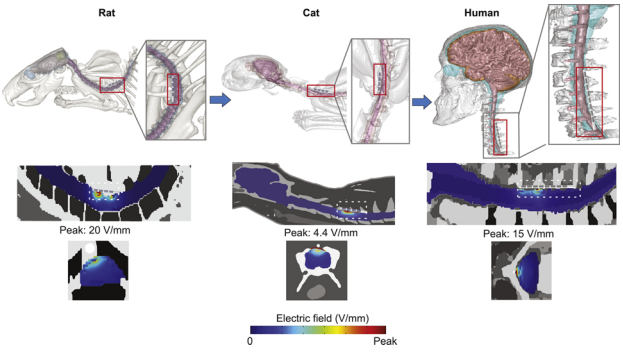

ARTICLE INFO

Keywords:
Spinal cord stimulation (SCS)
Quasi-uniform assumption
Electric field
Finite Element Model

ABSTRACT

Background: Quasi-uniform assumption is a general theory that postulates local electric field predicts neuronal activation. Computational current flow model of spinal cord stimulation (SCS) of humans and animal models inform how the quasi-uniform assumption can support scaling neuromodulation dose between humans and translational animal.
New method: Here we developed finite element models of cat and rat SCS, and brain slice, alongside SCS models. Boundary conditions related to species specific electrode dimensions applied, and electric fields per unit current (mA) predicted.
Results: Clinically and across animal, electric fields change abruptly over small distance compared to the neuronal morphology, such that each neuron is exposed to multiple electric fields. Per unit current, electric fields generally decrease with body mass, but not necessarily and proportionally across tissues. Peak electric field in dorsal column rat and cat were ~17x and ~1x of clinical values, for scaled electrodes and equal current. Within the spinal cord, the electric field for rat, cat, and human decreased to 50% of peak value caudo-rostrally (C5–C6) at 0.48 mm, 3.2 mm, and 8 mm, and mediolaterally at 0.14 mm, 2.3 mm, and 3.1 mm. Because these space constants are different, electric field across species cannot be matched without selecting a region of interest (ROI).
Comparison with existing method: This is the first computational model to support scaling neuromodulation dose between humans and translational animal.
Conclusions: Inter-species reproduction of the electric field profile across the entire surface of neuron populations is intractable. Approximating quasi-uniform electric field in a ROI is a rational step to translational scaling.

* Corresponding authors at: Department of Biomedical Engineering, The City College of New York, 85 Saint Nicholas Terrace, Rm 3366, New York, NY, 10031, USA.
E-mail addresses: nironzan@gmail.com, nkhadka@ccny.cuny.edu (N. Khadka), bikson@ccny.cuny.edu (M. Bikson).

https://doi.org/10.1016/j.jneumeth.2019.108446
Received 31 May 2019; Received in revised form 23 September 2019; Accepted 25 September 2019
Available online 04 October 2019
0165-0270/

1. Introduction

We extend the "quasi-uniform assumption" (Bikson et al., 2013) to apply it to animal models of spinal cord stimulation (SCS). For animal models of SCS to be meaningful, they must provide electrical stimulation in a way that approximates how the nervous system is activated during clinical therapy. Since the mechanisms of electrical stimulation are determined by which neuronal elements are excited (Ranck, 1975), SCS animal models would ideally use electrode montage (size, position) and current that stimulate the same distribution of neuronal elements as activated clinically. It is established that the spatial distribution of electric field across tissue (around neurons) determines which neuronal elements are excited (McIntyre and Grill, 1998; Rattay, 1999, 1986; Warman et al., 1992; Wongsarnpigoon and Grill, 2008), and so electrode montage and current in animal SCS models should create an electric field distribution approximating that produced clinically. However, this is impossible in practice, as animal anatomy is not proportionally scaled from humans. One can reproduce an electric field in one region of interest (e.g. the dorsal column of one segment), but not the exquisitely detailed electric field changes over space - which will be species (even animal) and dose specific.

This challenge in approximating electric field spatial distribution is not specific to SCS, but applies to all translational models of brain stimulation leading to the formulation of the quasi-uniform assumption (Bikson et al., 2013). The quasi-uniform assumption should be understood as practical tool, not an ideal solution. The quasi-uniform assumption relies on two logical steps. First, the quasi-uniform assumption deviates from the dogma of relying on activating function (the electric field derivative) in predicting neuronal excitation (McIntyre and Grill, 1999; Rattay, 1999), and rather suggests that most CNS neuronal elements will be excited directly by the local electric field (Arlotti et al., 2012; Rahman et al., 2013; Rubinstein, 1993; Tranchina and Nicholson, 1986). In fact, experiments and activation-function-based modeling already demonstrate polarization sensitivity directly to local electric field magnitude for neuronal elements such as axons terminals (synapses), dendrites, and compact neurons (see Discussion). Second, as the electric field varies in a complex manner across tissue that is inconsistent across species (Hurlbert and Tator, 1994; Idlett et al., 2019; Swiontek et al., 1976; Xu et al., 2017), the quasi-uniform assumption indicates identifying one region of interest (a nominal target) and matching the electric field in just that region across animal and clinical cases. Ironically, the more one argues again the first aspect (that only exquisitely detailed modeling of electric field gradients along each neuron, compartment is sufficient), the more the second aspect becomes required - since electric field changes across an entire single neuron, much less a population of neurons, cannot be reproduced between human and animal.

The spatio-temporal distribution of electric fields in the body determines stimulation outcomes. Under quasi-static assumptions (Bossetti et al., 2008), the temporal waveform is easy to replicate but the spatial distribution cannot be, where we can then find a basis in the quasi-uniform assumption.

There are three general approaches to scale stimulation dose in translational animal models. The first approach is to scale stimulation in the "dose space", namely to scale electrode size and/or current intensity by some arbitrary factor such as by animal size or physical space for the electrode. This approach is not principled (e.g. matching electrode current density between human and animal models does not produce equivalent outcomes; (Jackson et al., 2017)). The second approach is to use an acute physiological marker of nervous system activation (such as motor threshold; (Crosby et al., 2017, 2015a, 2015b; Guan et al., 2010; Koyama et al., 2018; Meuwissen et al., 2018; Prager, 2010; Sato et al., 2014; Schechtmann et al., 2008; Sdrulla et al., 2018; Song et al., 2013a, 2013b; Stiller et al., 1996; Yuan et al., 2014)) but using a stimulation waveform unlike that of interest for neuromodulation (e.g. using single pulse for motor threshold vs high rate pulse trains for neuromodulation). In this approach, the current is scaled based on this physiologic response, by the electrode montage is still ad hoc (e.g. what fits). Doing so ideally replicates in an animal model the neuronal elements (mechanism, and degree of activation) of a plausibly comparable acute physiological marker in human. However, the influence of stimulation other nervous system elements is not replicated, nor do the activated neuronal elements necessarily remain the same as waveform is changed. As a result, using an acute physiological maker to determine dose in animal is only valid as far as the acute physiological marker directly relates to the therapeutic mechanism.

The third approach to scale stimulation dose in translational animal models leverages computational models to predict electric fields (Bikson et al., 2015). In principle, this approach is based on long-standing principles that the electric field produced in the tissue along neuronal elements determines stimulation outcomes. But, our essential nuance to computational based modeling, which is the quasi-uniform assumption, is the reliance of electric field magnitude on one region of interest. The generalization of electric field magnitude as a predictor of neuronal activation is addressed in the Discussion. However, our central point here is more practical: if one wants to rely on tissue electric field as a mean to justify scaling in an animal model, than reliance of electric field is not just useful but realistically inevitable, including in translational SCS studies (Idlett et al., 2019). To make this point, we apply it in high-resolution models of rodent, cat, and human. Previous studies have modeled SCS clinically (Hernández-Labrado et al., 2011; Howell et al., 2014; Huang et al., 2014; Lee et al., 2011; Lempka et al., 2015) and in specific animal models (Capogrosso et al., 2013; Idlett et al., 2019; Xu et al., 2017)), and our approach here is not intended to be comprehensive (e.g. consider a wide range of electrode parameters) but rather reinforces these prior efforts in the context of the quasi-uniform assumption.

2. Materials and methods

We developed a computer-aided design (CAD) model of an exemplary brain slice chamber (din = 50 mm; dout = 60 mm; h = 40 mm), mimicking brain slice electric field stimulation (Bikson et al., 2004; Ghai et al., 2000; Gluckman et al., 1996) with two parallel conductive Ag/AgCl wire (d = 1 mm; l = 60 mm), and SCS leads in SolidWorks (Dassault Systemes Corp., MA, USA). For animal and human studies, we modelled two types of SCS leads namely a 4 Pt/Ir electrode contacts polyurethane SCS lead for animal study (rat: 1.35 mm electrode diameter, 3 mm electrode length, and 1 mm inter-electrode spacing; cat: 1.35 mm electrode diameter, 3 mm electrode length, and 1 mm inter-electrode spacing) and a 8 Pt/Ir electrode contacts SCS lead for human study (1.35 mm electrode diameter, 3 mm electrode length, and 1 mm inter-electrode spacing (Zannou et al., 2018)).

High resolution magnetic resonance imaging (MRI) scans of template healthy rat (0.1 mm), cat (0.1 mm), and human (0.8 mm) were segmented into tissue masks namely scalp, skull, csf, gray matter, white matter, cerebellum, hippocampus, thalamus, and air using Simpleware (Synopsys Inc., CA) by combining both automatic and manual morphological segmentation filters, and a volumetric FEM model was generated. SCS leads were then epidurally positioned over the targeted vertebrae level (lower cervical spine level and proximal to the mediolateral midline). We used voxel-based meshing algorithms which generated overly dense adaptive tetrahedral meshes of the brain slice chamber and the intricate animal models. The final mesh quality after multiple mesh refinements (within 1% error in voltage and current density at the spinal cord) was greater than 0.9 (COMSOL metric for mesh quality) indicating optimal elements in all models, and contained approximately 320000, 5950000, 22000000, 32200000 tetrahedral elements for slice chamber, rat, cat, and human model, respectively. The resulting volumetric meshes were later imported into COMSOL Multiphysics 5.1 (COMSOL Inc., MA, USA) to generate a finite element

method (FEM) models. The models were computationally solved using Laplace equation for electric current physics ($\nabla(\sigma\nabla V) = 0$), where V = potential and σ = conductivity) as field equation under stead-state assumption. Assigned material properties (electrical conductivities) for brain slice chamber, spinal tissues and electrode/lead were based on prior literature (Bikson et al., 2015; Song et al., 2015; Zannou et al., 2018).

In the brain slice chamber model, we simulated two parallel Ag/Agcl electrode placed laterally in a saline bath and applied normal current density equivalent to 1 mA ((J.n)* Areaanode = 1 mA) through one electrode (anode) while grounding the other electrode (cathode). The external boundaries of the brain slice chamber were electrically

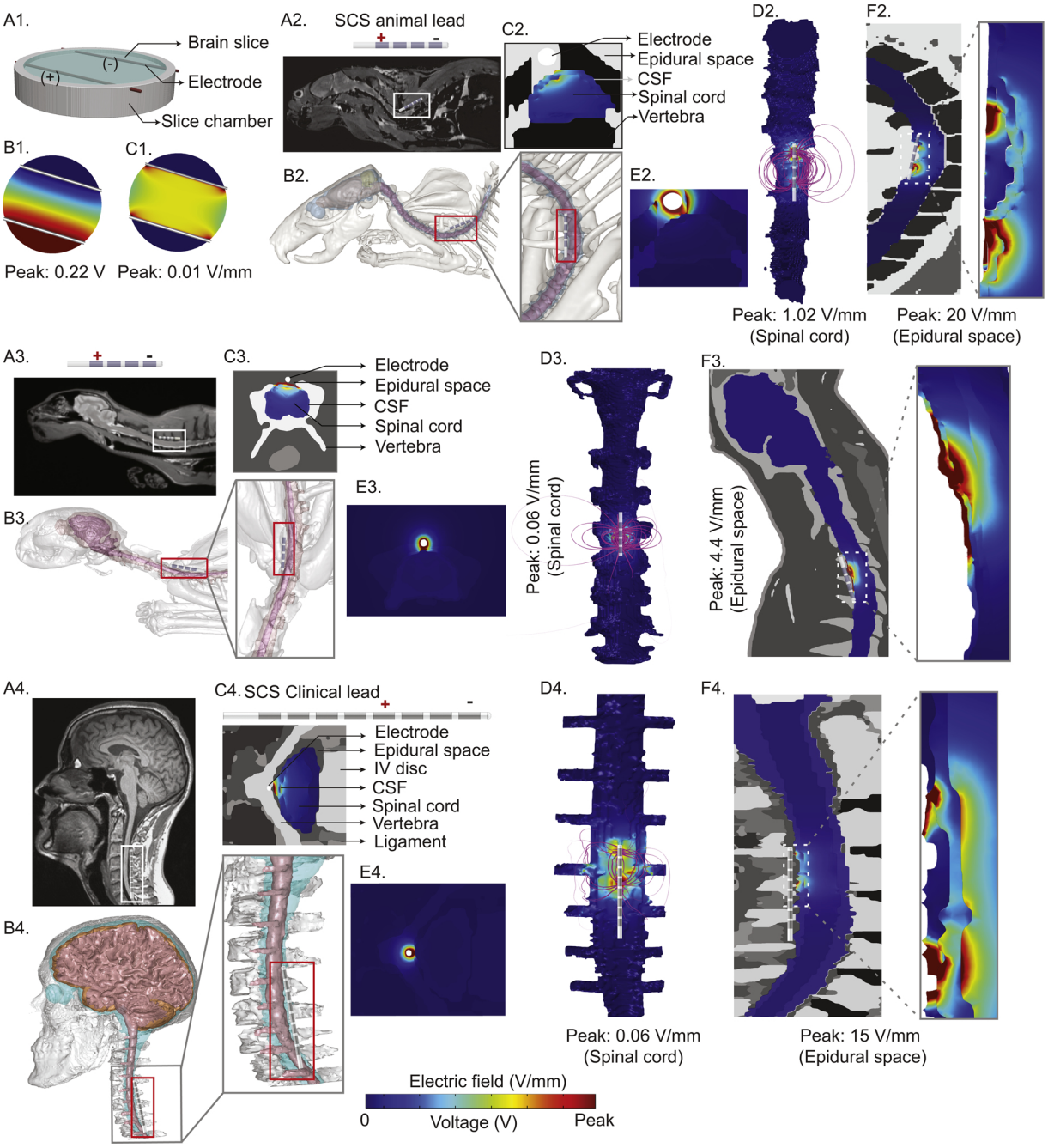

Fig. 1. Evaluation of the quasi-uniform assumption for SCS including brain slice, rat, cat, human, and clinical current flow simulation. We developed computer-aided design (CAD) model of a slice chamber, and a realistic MRI driven computational models of rat, cat, and human and predicted electric field and voltage across tissue. (A1) illustrates brain slice chamber with two parallel stimulating wires. (B1, C1) corresponding predicted peak voltage (0.22 V) and electric field intensity (0.01 V/mm) for the brain slice chamber in A1. (A2) MRI slice of a rat image with a SCS lead positioned epidurally along the lower cervical region. Segmented spinal cord tissues of the rat model (B2). (C2, D2) Cross-section view of predicted electric field and electric field streamlines plotted around the stimulating electrode contacts. (E2, F2) shows predicted peak electric field around the lead (epidural space: 20 V/mm) and the spinal cord (1.02 V/mm) respectively. (A3, B3, C3, D3, E3, F3) illustrates SCS lead positioning, segmentation, and electric field prediction in a cat FEM model. (A4) represents SCS lead positioning at the cervical vertebrae of a human FEM model. (B4) represents spinal cord tissue segmentation. (C4, E4) shows electric field distribution across spinal tissues. (D4) illustrates uniformly seeded electric field streamlines from the leads to the spinal cord (peak: 0.06 V/mm). (F4) represents predicted electric field in the epidural space (peak: 15 V/mm) and other peripheral spinal tissues. The key take-away of these predictions is not simply that peak electric field varies across species but that the spatial distribution of the electric field is complex and species specific, such that the electric field across species can only be matched in a selected ROI, not across all the spinal cord.

insulated (J.n = 0). In the rat, cat, and human SCS model, boundary conditions were applied in a bipolar configuration as: normal current density at the exposed boundary of E4 (anode: 1 mA), ground at the exposed surface of E1 (cathode), insulation on all other external surfaces of the spinal cord and the peripheral tissues, and continuity for internal boundaries. We set the relative tolerance (convergence criteria) of each model to 1 × 10-6 to get the most accurate solution while minimizing the errors. Corresponding voltage and electric fields were quantified from the simulations.

3. Results

Using exemplary computational models of the slice chamber with parallel electrodes and of rat, cat, and human with scaled cylindrical electrodes positioned epidurally over the targeted lower cervical vertebral column, the voltage and electric field intensity at the spinal cord and its peripheral tissues were predicted. Slice chamber FEM model predicted 0.22 V peak voltage and 0.01 V/mm electric field intensity. Predicted peak electric field around the lead (epidural space), csf, and spinal cord were 20, 7, and 1.02 V/mm, respectively for the rat model. For the cat model, predicted peak electric field intensity was 4.4, 0.14, and 0.06 V/mm at the epidural space, csf, and the spinal cord, respectively. Human SCS model predicted field intensities at the epidural space, csf and spinal cord of 15, 0.09, 0.06 V/mm respectively. Within the spinal cord, the electric field dropped to 50% of its peak intensity caudo-rostrally at 0.73 mm, 1.3 mm, and 1.5 mm and mediolaterally at 0.45 mm, 0.9 mm, and 0.85 mm distant from the peak intensity location for the rat, cat, and human respectively. The predicted electric field was only uniform in the slice chamber while, as expected, in the animal and human SCS the predicted electric field intensities were non-uniform - even on the scale of a single spinal neuron or axon (Hofstoetter et al., 2013; Holsheimer, 2002; Ladenbauer et al., 2010; Miranda et al., 2016; Rattay et al., 2000).

4. Discussion

The central proposition of this paper is that because it is not possible to reproduce the electric field distribution along diverse potential neuronal targets, the quasi-uniform assumption supports design and interpretation of animal models of SCS, (Fig. 1). A corollary of this proposition is the general applicability of considering the electric field magnitude as a meaningful predictor of neuronal activation. Each of these topics is considered separately below, but even to the extent detractors question the limits of the quasi-uniform assumption in general, then they acknowledge the limitations of translational animal models that necessitate this very assumption. The explicit goal of this paper is to explain the quasi-uniform assumption for translational animal research on spinal cord stimulation, with the broader and complex issue of general applicability addressed briefly (where an extended discussion beyond this paper scope). The computational models developed to illustrate the application of the quasi-uniform assumption largely confirm results from prior models (Holsheimer, 1998; Ladenbauer et al., 2010; Lempka et al., 2015; Miranda et al., 2016), and hardly capture the range of electrode configurations available; none-the-less they serve to show conventional notions of activating function are untenable in scaling dose between animal and human trials.

4.1. The quasi-uniform assumption in translational animal research

The quasi-uniform assumption (Bikson et al., 2015, 2013) is based on a proportional relationship between neuronal excitation and the local electric field magnitude (Arlotti et al., 2012; Rahman et al., 2013; Rubinstein, 1993; Tranchina and Nicholson, 1986). To the extent investigators aim to quantitively match tissue-level measures of electrical potency across human and animal models, the quasi-uniform assumption is required in translational animal studies of SCS. During SCS, the electric field varies in a complex manner across the spine (Fig. 1). It is not technically feasible in animal or brain slice studies to replicate the electric field in all regions of the spinal cord – since doing so would require applying a stimulation dose in given animal model that reproduces the voltage distribution across an arbitrarily large number of neuronal elements exactly as produced in human stimulation (despite gross difference in anatomy and cellular morphology). Since this is practically impossible, the solution is to select a clinical region of interest (e.g. dorsal horn at one segment level), predict the clinical electric field in that region of the spine, and then to replicate that electric field in an analogous region of the animal model. In selecting one electric field in a region of interest, the quasi-uniform assumption is applied. This approach was rigorously (implicitly) applied for an *ex vivo* mouse SCS model (Idlett et al., 2019).

There are two general alternatives to leveraging the quasi-uniform assumption. The first alternative is to scale electrode size and/or current applied by a factor related to an arbitrary measure of animal size. For example, using a 50-fold smaller electrode and/or 50-fold less current. But such approaches are not expected to produce comparable neuromodulation and are only as principled as the arbitrary scaling factors. It is not prudent to apply “smaller” stimulation (a smaller electrode and reduced applied current) heuristically because the resulting electric field may not be clinically meaningful in humans. The second alternative is, using an arbitrary electrode geometry, to titrate current intensity to produce an overt physiological response in an animal model – for example a motor response. This approach is underpinned by the assumption that grossly reproducing an overt physiological response that can be related to a clinical side-effect (e.g. motor twitch), will also reproduce a neuromodulation outcome in regard to a behavioral endpoint (e.g. reduction in pain) comparable to clinical SCS. This is only the case when the overt physiological outcome is the same pathway are the behavioral outcome or when the two are coincidentally related. Instead, one could identify the neuronal elements (e.g. dorsal column axon collaterals) that presumably underlie the desired behavioral outcome in humans (e.g. reduction in pain), and then provide stimulation in animal models to activate those same neuronal elements. This process therefore approximate tissue level influence which, for the reasons stated above, requires the quasi-uniform assumption.

The process of applying the quasi-uniform assumption is therefore: 1) identify the candidate neuronal element presumed responsible for the clinical outcome of interest; 2) using computational FEM model of current flow, simulate SCS dose in human (Fig. 1) to predict the peak electric field magnitude on those elements; 3) select a practical electrode geometry to be used in an animal model; 4) simulate the intensity applied to that electrode geometry to produce in the comparable neuronal element in the animal model as the electric field generated clinically (Fig. 1). For example, using the dorsal column as putative targets, for the specific electrode geometries considered in human and animal, we propose an intensity scaling factor of 17X and 1X to rat and cat. This workflow has limitations. Selecting which neuronal elements are relevant is an assumption, but a principled one that supports hypothesis testing. Special care is required in applying invasive microelectrode stimulation in animal studies precisely because they produce highly non-uniform fields near the electrodes which may produce local activation unrelated to the neuronal elements of translational interest.

4.2. The quasi-uniform assumption as a general marker of neurostimulation

There is a long-standing theoretical consideration of the role of electric field change along neuronal compartments, rather than simply electric field magnitude, to predict neuronal activation (Basser and Roth, 2000; Brocker and Grill, 2013; Ranck, 1975; Reilly et al., 1985). These conclusions derive from considering of long, uniform, straight peripheral axons subject to stimulation with proximal micro-electrodes (Frijns et al., 1994; Rubinstein and Spelman, 1988). This formalism has been extended to more complex neuronal geometries and macro-

electrode, including epidural spinal cord stimulation (Graham et al., 2019; Holsheimer, 1998; Howell et al., 2014; Kent et al., 2014; Khadka et al., 2019; Lee et al., 2011). But it is well accepted that an axon termination or bend (Arlotti et al., 2012; Chakraborty et al., 2018; McNeal, 1976; Mourdoukoutas et al., 2018; Rubinstein, 1993; Tranchina and Nicholson, 1986), an axon traversing tissues of sufficient different resistivities (Capogrosso et al., 2013; Danner et al., 2011; Ladenbauer et al., 2010; Miranda et al., 2007; Mourdoukoutas et al., 2018; Rattay et al., 2000; Struijk et al., 1993), and overall compact neuronal structures (Aberra et al., 2018; Chan et al., 1988; Radman et al., 2009b, 2009a; Struijk et al., 1993; Tranchina and Nicholson, 1986) will all effectively respond to the local electric field magnitude. Coburn (1985) notes "sharp turns in the path of the fiber itself can be equally influential [to extracellular potential changes] (Coburn, 1985)". Similarly noted is a characteristic feature of "dorsal column nerves fibers is the presence of myelinated collaterals perpendicular to the rostro-caudal fibers" such that activation by SCS is "significantly influenced by the presence of the collateral" (Struijk et al., 1992). Foundational texts on stimulation emphasize regions of curvature (e.g. bending of the spinal root) and changes in tissue environment (e.g. axons crossing from cerebrospinal fluid to white matter, or into the epidural space and vertebral bone) produce effective sensitivity to electric field magnitude (Rattay et al., 2000). The more detailed model precision, the more electric field magnitude dependent effects emerge. Finally, it is not simply that terminal polarization, bends, and other changes in morphology or environment track electric field magnitude, but to the extent that these regions are then the most sensitive to stimulation, they will determine activation threshold for the entire neuron.

Indeed, detailed experimental analysis of central stimulation in animals supports electric field-based mechanism. This includes *in vivo* data evaluation that the threshold current as a function of distance from stimulation electrode, where increase in threshold with the square of distance is consistent with electric field-based stimulation (Nowak and Bullier, 1996). This distance-threshold relationship is remarkably accurate and reproduced across CNS structures (Armstrong et al., 1973; Hentall et al., 1984; Marcus et al., 1979; Nowak and Bullier, 1996; Stoney et al., 1968), including spinal cord (Gustafsson and Jankowska, 1976; Jankowska and Roberts, 1972; Joucla et al., 2012; Stoney et al., 1968). This relationship is so well established that it has been used for decades, to characterize the cellular targets of stimulation (e.g. the "k" value; (Armstrong et al., 1973; Hentall et al., 1984; Kubin and Davies, 1988; Marcus et al., 1979; Nowak and Bullier, 1996; Yeomans et al., 1986)). Additionally, decades of *in vitro* data applying uniform electric field (with zero electric field gradient) have characterized neuromodulation including oscillations, synaptic processing, and plasticity (Bikson et al., 2004; Kronberg et al., 2017). Trancutaneous spinal cord stimulation may also rely on locally uniform electric fields (Danner et al., 2011; Lesperance et al., 2018; Priori et al., 2014).

Model driven optimization for non-invasive electrical stimulation has almost universally relied (implicitly) on the quasi-uniform assumption, including models for transcranial Direct Current Stimulation (tDCS; (Datta et al., 2009; Dmochowski et al., 2011)), transcranial Alternating Current Stimulation (tACS; (Rampersad et al., 2019; Reato et al., 2010)), and Transcranial Magnetic Stimulation (TMS; (Gomez et al., 2018; Thielscher et al., 2011)), Electroconvulsive Therapy (ECT; (Bai et al., 2017, 2012; Lee et al., 2016)) – with few notable deviations (Miranda et al., 2007; Salvador et al., 2011). In modeling deep brain stimulation, the quasi-uniform assumption has been leveraged (Astrom et al., 2015; Chaturvedi et al., 2010; Cubo et al., 2019) in cases of constrained optimization methodology or to avoid computational complexity (e.g. software for clinical practice). In most computational model of Spinal Cord Stimulation, non-uniform electric field is coupled to neuron morphology (Holsheimer, 2002; Lempka et al., 2019), though optimization or validation of new SCS approaches can rely on (quasi-uniform) electric field distribution. (Anderson et al., 2019; Coburn, 1985; Hernández-Labrado et al., 2011; Huang et al., 2014)

4.3. Inevitability of the quasi-uniform in translational animal models

None of this discussion should be taken to diminish the value of detailed SCS modeling which has become increasingly complex from pioneering work by Holsheimer et al. (Holsheimer and Struijk, 1991; Holsheimer and Wesselink, 1997) and Coburn and colleagues (Coburn, 1985, 1980) to contemporary efforts (Durá et al., 2019; Lempka et al., 2019, 2015; Min et al., 2014; Xu et al., 2017). When the functional models are used to prescribe optimal dose, it is an open question of how much does the detailed model verse (quasi-uniform) electric field-based analyses lead to distinct outcomes? With the latter lending themselves to closed-form (linear) optimization (Dmochowski et al., 2011) and fast (clinician toolbox) stimulation. Regardless, the scope of this paper is limited to consider the use of the quasi-uniform assumption in translational animal research. This, while the broader discussion about when polarization by electric field magnitude is relevant, we posit that the quasi-uniform assumption is not simply a principled, but an inevitable concept if tissue level electrical forces are to be rationally matched across specifics using computational models. As discussed, modeling and experimental studies support that in a complex 'soup' morphology, electric field magnitude indeed predicts maximal polarization (e.g. Eλ; (Rattay, 1986)) including compact neuron polarization (Joucla and Yvert, 2009), axon terminations (synapse) and bends (e.g. at roots). In any case, it is practically impossible to replicate SCS electric field changes across even a single hypothetical spinal neuron between species – much less across the entire population of neurons – make the quasi-uniform assumption a technical necessity in those translational animal models that want to relate tissue level measures of stimulation intensity. Ultimately, the question of when and how electric field magnitude can be used as a surrogate for neuromodulation efficacy in SCS is a broad and ambitious question, and the argument of this paper is only to present the quasi-uniform assumption as one tool to support meaningful translational studies on SCS.

Source(s) of financial support

This study was funded partially by grants to MB and JM from NIH (NIH-NIMH 1R01MH111896, NIH-NINDS 1R01NS101362, NIH-NCI U54CA137788/ U54CA132378, R03 NS054783) and New York State Department of Health (NYS DOH,DOH01-C31291GG).

The City University of New York (CUNY) has IP on neuro-stimulation systems and methods with authors Niranjan Khadka and Marom Bikson as inventors. MB has equity in Soterix Medical. MB serves on the advisory boards of Boston Scientific, Mecta, and GlaxoSmithKline Inc.

Declaration of Competing Interest

The City University of New York (CUNY) has IP on neuro-stimulation systems and methods with authors Niranjan Khadka and Marom Bikson as inventors. MB has equity in Soterix Medical. MB serves on the advisory boards of Boston Scientific, Mecta, and GlaxoSmithKline Inc.

References

Aberra, A.S., Peterchev, A.V., Grill, W.M., 2018. Biophysically realistic neuron models for simulation of cortical stimulation. J. Neural Eng. 15, 066023. https://doi.org/10.1088/1741-2552/aadbb1.

Anderson, D.J., Kipke, D.R., Nagel, S.J., Lempka, S.F., Machado, A.G., Holland, M.T., Gillies, G.T., Howard, M.A., Wilson, S., 2019. Intradural spinal cord stimulation: performance modeling of a new modality. Front. Neurosci. 13, 253. https://doi.org/10.3389/fnins.2019.00253.

Arlotti, M., Rahman, A., Minhas, P., Bikson, M., 2012. Axon terminal polarization induced by weak uniform DC electric fields: a modeling study. Conf. Proc. IEEE Eng. Med. Biol. Soc. 2012, 4575–4578. https://doi.org/10.1109/EMBC.2012.6346985.

Armstrong, D.M., Harvey, R.J., Schild, R.F., 1973. The spatial organisation of climbing fibre branching in the cat cerebellum. Exp. Brain Res. 18, 40–58.

Astrom, M., Diczfalusy, E., Martens, H., Wardell, K., 2015. Relationship between neural activation and electric field distribution during deep brain stimulation. IEEE Trans. Biomed. Eng. 62, 664–672. https://doi.org/10.1109/TBME.2014.2363494.

Bai, S., Gálvez, V., Dokos, S., Martin, D., Bikson, M., Loo, C., 2017. Computational models of Bitemporal, Bifrontal and Right Unilateral ECT predict differential stimulation of brain regions associated with efficacy and cognitive side effects. Eur. Psychiatry 41, 21–29. https://doi.org/10.1016/j.eurpsy.2016.09.005.

Bai, S., Loo, C., Al Abed, A., Dokos, S., 2012. A computational model of direct brain excitation induced by electroconvulsive therapy: comparison among three conventional electrode placements. Brain Stimul. 5, 408–421. https://doi.org/10.1016/j.brs.2011.07.004.

Basser, P.J., Roth, B.J., 2000. New currents in electrical stimulation of excitable tissues. Annu. Rev. Biomed. Eng. 2, 377–397. https://doi.org/10.1146/annurev.bioeng.2.1.377.

Bikson, M., Dmochowski, J., Rahman, A., 2013. The “quasi-uniform” assumption in animal and computational models of non-invasive electrical stimulation. Brain Stimul. 6, 704–705. https://doi.org/10.1016/j.brs.2012.11.005.

Bikson, M., Inoue, M., Akiyama, H., Deans, J.K., Fox, J.E., Miyakawa, H., Jefferys, J.G.R., 2004. Effects of uniform extracellular DC electric fields on excitability in rat hippocampal slices in vitro. J. Physiol. (Lond.) 557, 175–190. https://doi.org/10.1113/jphysiol.2003.055772.

Bikson, M., Truong, D.Q., Mourdoukoutas, A.P., Aboseria, M., Khadka, N., Adair, D., Rahman, A., 2015. Modeling sequence and quasi-uniform assumption in computational neurostimulation. Prog. Brain Res. 222, 1–23. https://doi.org/10.1016/bs.pbr.2015.08.005.

Bossetti, C.A., Birdno, M.J., Grill, W.M., 2008. Analysis of the quasi-static approximation for calculating potentials generated by neural stimulation. J. Neural Eng. 5, 44–53. https://doi.org/10.1088/1741-2560/5/1/005.

Brocker, D.T., Grill, W.M., 2013. Chapter 1 - principles of electrical stimulation of neural tissue. In: Lozano, A.M., Hallett, M. (Eds.), Handbook of Clinical Neurology, Brain Stimulation. Elsevier, pp. 3–18. https://doi.org/10.1016/B978-0-444-53497-2.00001-2.

Capogrosso, M., Wenger, N., Raspopovic, S., Musienko, P., Beauparlant, J., Luciani, L.B., Courtine, G., Micera, S., 2013. A computational model for epidural electrical stimulation of spinal sensorimotor circuits. J. Neurosci. 33, 19326–19340. https://doi.org/10.1523/JNEUROSCI.1688-13.2013.

Chakraborty, D., Truong, D.Q., Bikson, M., Kaphzan, H., 2018. Neuromodulation of axon terminals. Cereb. Cortex 28, 2786–2794. https://doi.org/10.1093/cercor/bhx158.

Chan, C.Y., Hounsgaard, J., Nicholson, C., 1988. Effects of electric fields on transmembrane potential and excitability of turtle cerebellar Purkinje cells in vitro. J. Physiol. (Lond.) 402, 751–771. https://doi.org/10.1113/jphysiol.1988.sp017232.

Chaturvedi, A., Butson, C.R., Lempka, S.F., Cooper, S.E., McIntyre, C.C., 2010. Patient-specific models of deep brain stimulation: influence of field model complexity on neural activation predictions. Brain Stimul. 3, 65–67. https://doi.org/10.1016/j.brs.2010.01.003.

Coburn, B., 1985. A theoretical study of epidural electrical stimulation of the spinal cord–part II: effects on long myelinated fibers. IEEE Trans. Biomed. Eng. 32, 978–986. https://doi.org/10.1109/TBME.1985.325649.

Coburn, B., 1980. Electrical stimulation of the spinal cord: two-dimensional finite element analysis with particular reference to epidural electrodes. Med. Biol. Eng. Comput. 18, 573–584. https://doi.org/10.1007/bf02443129.

Crosby, N.D., Goodman Keiser, M.D., Smith, J.R., Zeeman, M.E., Winkelstein, B.A., 2015a. Stimulation parameters define the effectiveness of burst spinal cord stimulation in a rat model of neuropathic pain. Neuromodulation 18, 1–8. https://doi.org/10.1111/ner.12221. discussion 8.

Crosby, N.D., Janik, J.J., Grill, W.M., 2017. Modulation of activity and conduction in single dorsal column axons by kilohertz-frequency spinal cord stimulation. J. Neurophysiol. 117, 136–147. https://doi.org/10.1152/jn.00701.2016.

Crosby, N.D., Weisshaar, C.L., Smith, J.R., Zeeman, M.E., Goodman-Keiser, M.D., Winkelstein, B.A., 2015b. Burst and tonic spinal cord stimulation differentially activate GABAergic mechanisms to attenuate pain in a rat model of cervical radiculopathy. IEEE Trans. Biomed. Eng. 62, 1604–1613. https://doi.org/10.1109/TBME.2015.2399374.

Cubo, R., Fahlström, M., Jiltsova, E., Andersson, H., Medvedev, A., 2019. Calculating deep brain stimulation amplitudes and power consumption by constrained optimization. J. Neural Eng. 16, 016020. https://doi.org/10.1088/1741-2552/aaeeb7.

Danner, S.M., Hofstoetter, U.S., Ladenbauer, J., Rattay, F., Minassian, K., 2011. Can the human lumbar posterior columns be stimulated by transcutaneous spinal cord stimulation? A modeling study. Artif. Organs 35, 257–262. https://doi.org/10.1111/j.1525-1594.2011.01213.x.

Datta, A., Bansal, V., Diaz, J., Patel, J., Reato, D., Bikson, M., 2009. Gyri-precise head model of transcranial direct current stimulation: improved spatial focality using a ring electrode versus conventional rectangular pad. Brain Stimul. 2 (201–207), 207. https://doi.org/10.1016/j.brs.2009.03.005. e1.

Dmochowski, J.P., Datta, A., Bikson, M., Su, Y., Parra, L.C., 2011. Optimized multi-electrode stimulation increases focality and intensity at target. J. Neural Eng. 8, 046011. https://doi.org/10.1088/1741-2560/8/4/046011.

Durá, J.L., Solanes, C., De Andrés, J., Saiz, J., 2019. Computational study of the effect of electrode polarity on neural activation related to paresthesia coverage in spinal cord stimulation therapy. Neuromodulation 22, 269–279. https://doi.org/10.1111/ner.12909.

Frijns, J.H., Mooij, J., ten Kate, J.H., 1994. A quantitative approach to modeling mammalian myelinated nerve fibers for electrical prosthesis design. IEEE Trans. Biomed. Eng. 41, 556–566. https://doi.org/10.1109/10.293243.

Ghai, R.S., Bikson, M., Durand, D.M., 2000. Effects of applied electric fields on low-calcium epileptiform activity in the CA1 region of rat hippocampal slices. J. Neurophysiol. 84, 274–280. https://doi.org/10.1152/jn.2000.84.1.274.

Gluckman, B.J., Neel, E.J., Netoff, T.I., Ditto, W.L., Spano, M.L., Schiff, S.J., 1996. Electric field suppression of epileptiform activity in hippocampal slices. J. Neurophysiol. 76, 4202–4205. https://doi.org/10.1152/jn.1996.76.6.4202.

Gomez, L.J., Goetz, S.M., Peterchev, A.V., 2018. Design of transcranial magnetic stimulation coils with optimal trade-off between depth, focality, and energy. J. Neural Eng. 15, 046033. https://doi.org/10.1088/1741-2552/aac967.

Graham, R.D., Bruns, T.M., Duan, B., Lempka, S.F., 2019. Dorsal root ganglion stimulation for chronic pain modulates Aβ-fiber activity but not C-fiber activity: a computational modeling study. Clin. Neurophysiol. https://doi.org/10.1016/j.clinph.2019.02.016.

Guan, Y., Wacnik, P.W., Yang, F., Carteret, A.F., Chung, C.-Y., Meyer, R.A., Raja, S.N., 2010. Spinal cord stimulation-induced AnalgesiaElectrical stimulation of dorsal column and dorsal roots attenuates dorsal horn neuronal excitability in neuropathic rats. Anesthes 113, 1392–1405. https://doi.org/10.1097/ALN.0b013e3181fcd95c.

Gustafsson, B., Jankowska, E., 1976. Direct and indirect activation of nerve cells by electrical pulses applied extracellularly. J. Physiol. (Lond.) 258, 33–61. https://doi.org/10.1113/jphysiol.1976.sp011405.

Hentall, I.D., Zorman, G., Kansky, S., Fields, H.L., 1984. Relations among threshold, spike height, electrode distance, and conduction velocity in electrical stimulation of certain medullospinal neurons. J. Neurophysiol. 51, 968–977. https://doi.org/10.1152/jn.1984.51.5.968.

Hernández-Labrado, G.R., Polo, J.L., López-Dolado, E., Collazos-Castro, J.E., 2011. Spinal cord direct current stimulation: finite element analysis of the electric field and current density. Med. Biol. Eng. Comput. 49, 417–429. https://doi.org/10.1007/s11517-011-0756-9.

Hofstoetter, U.S., Danner, S.M., Minassian, K., 2013. Paraspinal magnetic and transcutaneous electrical stimulation. In: Jaeger, D., Jung, R. (Eds.), Encyclopedia of Computational Neuroscience. Springer New York, New York, NY, pp. 1–21.

Holsheimer, J., 2002. Which neuronal elements are activated directly by spinal cord stimulation. Neuromodulation 5, 25–31. https://doi.org/10.1046/j.1525-1403.2002._2005.x.

Holsheimer, J., 1998. Computer modelling of spinal cord stimulation and its contribution to therapeutic efficacy. Spinal Cord 36, 531–540.

Holsheimer, J., Struijk, J.J., 1991. How do geometric factors influence epidural spinal cord stimulation? A quantitative analysis by computer modeling. Stereotact. Funct. Neurosurg. 56, 234–249. https://doi.org/10.1159/000099410.

Holsheimer, J., Wesselink, W.A., 1997. Optimum electrode geometry for spinal cord stimulation: the narrow bipole and tripole. Med. Biol. Eng. Comput. 35, 493–497. https://doi.org/10.1007/BF02525529.

Howell, B., Lad, S.P., Grill, W.M., 2014. Evaluation of intradural stimulation efficiency and selectivity in a computational model of spinal cord stimulation. PLoS One 9, e114938. https://doi.org/10.1371/journal.pone.0114938.

Huang, Q., Oya, H., Flouty, O.E., Reddy, C.G., Howard, M.A., Gillies, G.T., Utz, M., 2014. Comparison of spinal cord stimulation profiles from intra- and extradural electrode arrangements by finite element modelling. Med. Biol. Eng. Comput. 52, 531–538. https://doi.org/10.1007/s11517-014-1157-7.

Hurlbert, R.J., Tator, C.H., 1994. Characterization of longitudinal field gradients from electrical stimulation in the normal and injured rodent spinal cord. Neurosurgery 34, 471–482. https://doi.org/10.1227/00006123-199403000-00013. discussion 482-483.

Idlett, S.L., Halder, M., Zhang, T., Quevedo, J.N., Brill, N., Gu, W., Moffitt, M.A., Hochman, S., 2019. Assessment of axonal recruitment using model-guided preclinical spinal cord stimulation in the ex vivo adult mouse spinal cord. J. Neurophysiol. https://doi.org/10.1152/jn.00538.2018.

Jackson, M.P., Bikson, M., Liebetanz, D., Nitsche, M., 2017. How to consider animal data in tDCS safety standards. Brain Stimul. 10, 1141–1142. https://doi.org/10.1016/j.brs.2017.08.004.

Jankowska, E., Roberts, W.J., 1972. An electrophysiological demonstration of the axonal projections of single spinal interneurones in the cat. J. Physiol. (Paris) 222, 597–622.

Joucla, S., Branchereau, P., Cattaert, D., Yvert, B., 2012. Extracellular neural microstimulation may activate much larger regions than expected by simulations: a combined experimental and modeling study. PLoS One 7, e41324. https://doi.org/10.1371/journal.pone.0041324.

Joucla, S., Yvert, B., 2009. The “mirror” estimate: an intuitive predictor of membrane polarization during extracellular stimulation. Biophys. J. 96, 3495–3508. https://doi.org/10.1016/j.bpj.2008.12.3961.

Kent, A.R., Min, X., Rosenberg, S.P., Fayram, T.A., 2014. Computational modeling analysis of a spinal cord stimulation paddle lead reveals broad, gapless dermatomal coverage. 2014 36th Annual International Conference of the IEEE Engineering in Medicine and Biology Society. Presented at the 2014 36th Annual International Conference of the IEEE Engineering in Medicine and Biology Society 6254–6257. https://doi.org/10.1109/EMBC.2014.6945058.

Khadka, N., Zannou, A., Truong, D., Zhang, T., Esteller, R., Hersey, B., Bikson, M., 2019. Generation 2 kilohertz spinal cord stimulation (kHz-SCS) bioheat multi-physics model. Brain Stimul. 12, 566. https://doi.org/10.1016/j.brs.2018.12.876.

Koyama, S., Xia, J., Leblanc, B.W., Gu, J.W., Saab, C.Y., 2018. Sub-paresthesia spinal cord stimulation reverses thermal hyperalgesia and modulates low frequency EEG in a rat model of neuropathic pain. Sci. Rep. 8, 7181. https://doi.org/10.1038/s41598-018-25420-w.

Kronberg, G., Bridi, M., Abel, T., Bikson, M., Parra, L.C., 2017. Direct current stimulation modulates LTP and LTD: activity dependence and dendritic effects. Brain Stimul. 10, 51–58. https://doi.org/10.1016/j.brs.2016.10.001.

Kubin, L., Davies, R.O., 1988. Sites of termination and relay of pulmonary rapidly adapting receptors as studied by spike-triggered averaging. Brain Res. 443, 215–221.

Ladenbauer, J., Minassian, K., Hofstoetter, U.S., Dimitrijevic, M.R., Rattay, F., 2010.

Stimulation of the human lumbar spinal cord with implanted and surface electrodes: a computer simulation study. IEEE Trans. Neural Syst. Rehabil. Eng. 18, 637–645. https://doi.org/10.1109/TNSRE.2010.2054112.
Lee, D., Hershey, B., Bradley, K., Yearwood, T., 2011. Predicted effects of pulse width programming in spinal cord stimulation: a mathematical modeling study. Med. Biol. Eng. Comput. 49, 765. https://doi.org/10.1007/s11517-011-0780-9.
Lee, W.H., Lisanby, S.H., Laine, A.F., Peterchev, A.V., 2016. Comparison of electric field strength and spatial distribution of electroconvulsive therapy and magnetic seizure therapy in a realistic human head model. Eur. Psychiatry 36, 55–64. https://doi.org/10.1016/j.eurpsy.2016.03.003.
Lempka, S.F., McIntyre, C.C., Kilgore, K.L., Machado, A.G., 2015. Computational analysis of kilohertz frequency spinal cord stimulation for chronic pain management. Anesthesiology 122, 1362–1376. https://doi.org/10.1097/ALN.0000000000000649.
Lempka, S.F., Zander, H.J., Anaya, C.J., Wyant, A., Ozinga, J.G., Machado, A.G., 2019. Patient-specific analysis of neural activation during spinal cord stimulation for pain. Neuromodulation. https://doi.org/10.1111/ner.13037.
Lesperance, L.S., Lankarany, M., Zhang, T.C., Esteller, R., Ratté, S., Prescott, S.A., 2018. Artifactual hyperpolarization during extracellular electrical stimulation: proposed mechanism of high-rate neuromodulation disproved. Brain Stimul. 11, 582–591. https://doi.org/10.1016/j.brs.2017.12.004.
Marcus, S., Zarzecki, P., Asanuma, H., 1979. An estimate of effective spread of stimulating current. Exp. Brain Res. 34, 68–72.
McIntyre, C.C., Grill, W.M., 1999. Excitation of central nervous system neurons by non-uniform electric fields. Biophys. J. 76, 878–888. https://doi.org/10.1016/S0006-3495(99)77251-6.
McIntyre, C.C., Grill, W.M., 1998. Sensitivity analysis of a model of mammalian neural membrane. Biol. Cybern. 79, 29–37. https://doi.org/10.1007/s004220050455.
McNeal, D.R., 1976. Analysis of a model for excitation of myelinated nerve. IEEE Trans. Biomed. Eng. 23, 329–337.
Meuwissen, K.P.V., Gu, J.W., Zhang, T.C., Joosten, E.A.J., 2018. Conventional-SCS vs. Burst-SCS and the behavioral effect on mechanical hypersensitivity in a rat model of chronic neuropathic pain: effect of amplitude. Neuromodulation 21, 19–30. https://doi.org/10.1111/ner.12731.
Min, X., Kent, A.R., Rosenberg, S.P., Fayram, T.A., 2014. Modeling dermatome selectivity of single-and multiple-current source spinal cord stimulation systems. Conf. Proc. IEEE Eng. Med. Biol. Soc. 2014, 6246–6249. https://doi.org/10.1109/EMBC.2014.6945056.
Miranda, P.C., Correia, L., Salvador, R., Basser, P.J., 2007. Tissue heterogeneity as a mechanism for localized neural stimulation by applied electric fields. Phys. Med. Biol. 52, 5603–5617. https://doi.org/10.1088/0031-9155/52/18/009.
Miranda, P.C., Salvador, R., Wenger, C., Fernandes, S.R., 2016. Computational models of non-invasive brain and spinal cord stimulation. 2016 38th Annual International Conference of the IEEE Engineering in Medicine and Biology Society (EMBC). Presented at the 2016 38th Annual International Conference of the IEEE Engineering in Medicine and Biology Society (EMBC) 6457–6460. https://doi.org/10.1109/EMBC.2016.7592207.
Mourdoukoutas, A.P., Truong, D.Q., Adair, D.K., Simon, B.J., Bikson, M., 2018. High-resolution multi-scale computational model for non-invasive cervical vagus nerve stimulation. Neuromodulation 21, 261–268. https://doi.org/10.1111/ner.12706.
Nowak, L.G., Bullier, J., 1996. Spread of stimulating current in the cortical grey matter of rat visual cortex studied on a new in vitro slice preparation. J. Neurosci. Methods 67, 237–248.
Prager, J.P., 2010. What does the mechanism of spinal cord stimulation tell us about complex regional pain syndrome? Pain Med. 11, 1278–1283. https://doi.org/10.1111/j.1526-4637.2010.00915.x.
Priori, A., Ciocca, M., Parazzini, M., Vergari, M., Ferrucci, R., 2014. Transcranial cerebellar direct current stimulation and transcutaneous spinal cord direct current stimulation as innovative tools for neuroscientists. J. Physiol. (Paris) 592, 3345–3369. https://doi.org/10.1113/jphysiol.2013.270280.
Radman, T., Datta, A., Ramos, R.L., Brumberg, J.C., Bikson, M., 2009a. One-dimensional representation of a neuron in a uniform electric field. Conf. Proc. IEEE Eng. Med. Biol. Soc. 2009, 6481–6484. https://doi.org/10.1109/IEMBS.2009.5333586.
Radman, T., Ramos, R.L., Brumberg, J.C., Bikson, M., 2009b. Role of cortical cell type and morphology in subthreshold and suprathreshold uniform electric field stimulation in vitro. Brain Stimul. 2 (215–228), 228. https://doi.org/10.1016/j.brs.2009.03.007.e1–3.
Rahman, A., Reato, D., Arlotti, M., Gasca, F., Datta, A., Parra, L.C., Bikson, M., 2013. Cellular effects of acute direct current stimulation: somatic and synaptic terminal effects. J. Physiol. (Lond.) 591, 2563–2578. https://doi.org/10.1113/jphysiol.2012.247171.
Rampersad, S., Roig-Solvas, B., Yarossi, M., Kulkarni, P.P., Santarnecchi, E., Dorval, A.D., Brooks, D.H., 2019. Prospects for transcranial temporal interference stimulation in humans: a computational study. Neuroimage, 116124. https://doi.org/10.1016/j.neuroimage.2019.116124.
Ranck, J.B., 1975. Which elements are excited in electrical stimulation of mammalian central nervous system: a review. Brain Res. 98, 417–440.
Rattay, F., 1999. The basic mechanism for the electrical stimulation of the nervous system. Neuroscience 89, 335–346.
Rattay, F., 1986. Analysis of models for external stimulation of axons. IEEE Trans. Biomed. Eng. 33, 974–977. https://doi.org/10.1109/TBME.1986.325670.
Rattay, F., Minassian, K., Dimitrijevic, M.R., 2000. Epidural electrical stimulation of posterior structures of the human lumbosacral cord: 2. Quantitative analysis by computer modeling. Spinal Cord 38, 473–489.
Reato, D., Rahman, A., Bikson, M., Parra, L.C., 2010. Low-intensity electrical stimulation affects network dynamics by modulating population rate and spike timing. J. Neurosci. 30, 15067–15079. https://doi.org/10.1523/JNEUROSCI.2059-10.2010.
Reilly, J.P., Freeman, V.T., Larkin, W.D., 1985. Sensory effects of transient electrical stimulation–evaluation with a neuroelectric model. IEEE Trans. Biomed. Eng. 32, 1001–1011. https://doi.org/10.1109/TBME.1985.325509.
Rubinstein, J.T., 1993. Axon termination conditions for electrical stimulation. IEEE Trans. Biomed. Eng. 40, 654–663. https://doi.org/10.1109/10.237695.
Rubinstein, J.T., Spelman, F.A., 1988. Analytical theory for extracellular electrical stimulation of nerve with focal electrodes. I. Passive unmyelinated axon. Biophys. J. 54, 975–981. https://doi.org/10.1016/S0006-3495(88)83035-2.
Salvador, R., Silva, S., Basser, P.J., Miranda, P.C., 2011. Determining which mechanisms lead to activation in the motor cortex: a modeling study of transcranial magnetic stimulation using realistic stimulus waveforms and sulcal geometry. Clin. Neurophysiol. 122, 748–758. https://doi.org/10.1016/j.clinph.2010.09.022.
Sato, K.L., Johanek, L.M., Sanada, L.S., Sluka, K.A., 2014. Spinal cord stimulation reduces mechanical hyperalgesia and glial cell activation in animals with neuropathic pain. Anesth. Analg. 118, 464–472. https://doi.org/10.1213/ANE.0000000000000047.
Schechtmann, G., Song, Z., Ultenius, C., Meyerson, B.A., Linderoth, B., 2008. Cholinergic mechanisms involved in the pain relieving effect of spinal cord stimulation in a model of neuropathy. PAIN 139, 136–145. https://doi.org/10.1016/j.pain.2008.03.023.
Sdrulla, A.D., Guan, Y., Raja, S.N., 2018. Spinal cord stimulation: clinical efficacy and potential mechanisms. Pain Pract. 18, 1048–1067. https://doi.org/10.1111/papr.12692.
Song, W., Truong, D.Q., Bikson, M., Martin, J.H., 2015. Transspinal direct current stimulation immediately modifies motor cortex sensorimotor maps. J. Neurophysiol. 113, 2801–2811. https://doi.org/10.1152/jn.00784.2014.
Song, Z., Ansah, O.B., Meyerson, B.A., Pertovaara, A., Linderoth, B., 2013a. The rostroventromedial medulla is engaged in the effects of spinal cord stimulation in a rodent model of neuropathic pain. Neuroscience 247, 134–144. https://doi.org/10.1016/j.neuroscience.2013.05.027.
Song, Z., Ansah, O.B., Meyerson, B.A., Pertovaara, A., Linderoth, B., 2013b. Exploration of supraspinal mechanisms in effects of spinal cord stimulation: role of the locus coeruleus. Neuroscience 253, 426–434. https://doi.org/10.1016/j.neuroscience.2013.09.006.
Stiller, C.O., Cui, J.G., O'Connor, W.T., Brodin, E., Meyerson, B.A., Linderoth, B., 1996. Release of gamma-aminobutyric acid in the dorsal horn and suppression of tactile allodynia by spinal cord stimulation in mononeuropathic rats. Neurosurgery 39, 367–374. https://doi.org/10.1097/00006123-199608000-00026. discussion 374-375.
Stoney, S.D., Thompson, W.D., Asanuma, H., 1968. Excitation of pyramidal tract cells by intracortical microstimulation: effective extent of stimulating current. J. Neurophysiol. 31, 659–669. https://doi.org/10.1152/jn.1968.31.5.659.
Struijk, J.J., Holsheimer, J., Boom, H.B.K., 1993. Excitation of dorsal root fibers in spinal cord stimulation: a theoretical study. IEEE Trans. Biomed. Eng. 40, 632–639. https://doi.org/10.1109/10.237693.
Struijk, J.J., Holsheimer, J., van der Heide, G.G., Boom, H.B., 1992. Recruitment of dorsal column fibers in spinal cord stimulation: influence of collateral branching. IEEE Trans. Biomed. Eng. 39, 903–912. https://doi.org/10.1109/10.256423.
Swiontek, T.J., Sances, A., Larson, S.J., Ackmann, J.J., Cusick, J.F., Meyer, G.A., Millar, E.A., 1976. Spinal cord implant studies. IEEE Trans. Biomed. Eng. 23, 307–312. https://doi.org/10.1109/tbme.1976.324590.
Thielscher, A., Opitz, A., Windhoff, M., 2011. Impact of the gyral geometry on the electric field induced by transcranial magnetic stimulation. NeuroImage 54, 234–243. https://doi.org/10.1016/j.neuroimage.2010.07.061.
Tranchina, D., Nicholson, C., 1986. A model for the polarization of neurons by extrinsically applied electric fields. Biophys. J. 50, 1139–1156. https://doi.org/10.1016/S0006-3495(86)83558-5.
Warman, E.N., Grill, W.M., Durand, D., 1992. Modeling the effects of electric fields on nerve fibers: determination of excitation thresholds. IEEE Trans. Biomed. Eng. 39, 1244–1254.
Wongsarnpigoon, A., Grill, W.M., 2008. Computational modeling of epidural cortical stimulation. J. Neural Eng. 5, 443–454. https://doi.org/10.1088/1741-2560/5/4/009.
Xu, Q., Kong, L., Zhou, H., He, J., 2017. Epidural stimulation of rat spinal cord at lumbosacral segment using a surface electrode: a computer simulation study. IEEE Trans. Neural Syst. Rehabil. Eng. 25, 1763–1772. https://doi.org/10.1109/TNSRE.2016.2625312.
Yeomans, J., Prior, P., Bateman, F., 1986. Current-distance relations of axons mediating circling elicited by midbrain stimulation. Brain Res. 372, 95–106. https://doi.org/10.1016/0006-8993(86)91462-9.
Yuan, B., Liu, D., Liu, X., 2014. Spinal cord stimulation exerts analgesia effects in chronic constriction injury rats via suppression of the TLR4/NF-κB pathway. Neurosci. Lett. 581, 63–68. https://doi.org/10.1016/j.neulet.2014.08.023.
Zannou, A.L., Khadka, N., Truong, D.Q., Zhang, T., Esteller, R., Hershey, B., Bikson, M., 2018. Temperature increases by kilohertz frequency spinal cord stimulation. Brain Stimul. https://doi.org/10.1016/j.brs.2018.10.007.